Structure and Chemistry of Chemisorbed PF_3, PF_2, and PF on Ni(111): An ESDIAD Study

Mark D. Alvey and John T. Yates, Jr.*

Contribution from the Surface Science Center, Department of Chemistry, University of Pittsburgh, Pittsburgh, Pennsylvania 15260. *Received July 17, 1987*

Abstract: The chemisorption of PF_3 on Ni(111) was studied with the electron stimulated desorption ion angular distribution (ESDIAD) technique, temperature programmed desorption (TPD), Auger electron spectroscopy (AES), and low energy electron diffraction (LEED). PF_3 is shown to bond to atop Ni sites, with PF bonds azimuthally oriented over neighboring Ni atoms. There are two such orientations on the Ni(111) surface that contribute to the observed six beam F^+ ESDIAD pattern. Also, PF_3(ads) dissociates under electron irradiation, producing the surface species PF_2(ads) and PF(ads). The PF_2 and PF species produce a F^+ ESDIAD pattern which indicates that PF_2 is bound to 2-fold bridge sites, and PF is bound so that the P-F bond is normal to the surface. The chemisorption bonding of PF_3 and PF_2 to Ni(111) is in accordance with known modes of coordination of these ligands in transition-metal complexes.

1. Introduction

Traditionally, chemisorption at metal surfaces has been linked with concepts that also apply to bonding in mono- or multimetal compounds. This analogy serves as a link between studies of chemisorption on metals and the large body of inorganic chemistry literature and provides suggestions as to which chemisorption systems will be interesting to study.[1]

PF_3 is an interesting molecule because of its electronic structure that allows donation of charge to a metal atom through the PF_3 ($8a_1$) orbital and back-bonding from the metal d orbitals into the PF_3 (7e) orbital[2] (the 7e orbital is an antibonding orbital that consists of p and d orbitals on the phosphorus atom[2]). The chemistry of PF_3 has been extensively reviewed by Nixon,[2] who also briefly mentions surface studies with PF_3.

As far as the authors are aware, the first study of PF_3 on a surface was performed by Blyholder and Sheets[3] where PF_3 was adsorbed on to metal clusters supported in oil. They observed, by infrared spectroscopy, evidence of back-donation into the 7e orbital. Ertl et al., in studies of PF_3 adsorption on Fe(110), conclude that the bonding of PF_3 is analogous to that of PF_3 in mononuclear transition-metal complexes.[4] Nitschke et al.[5] have used ultraviolet photoelectron spectroscopy (UPS) and LEED to study properties of adsorbed PF_3 on Ni(111). They see that a σ-donor–π-acceptor model for PF_3 bonding is consistent with their results. Most notably, they observe that PF_3 does not decompose below 400 K and a PF_3 overlayer produces a p(2×2) low energy electron diffraction (LEED) pattern that is unstable in the electron beam, and they argue that PF_3 does not bond in multiply coordinated sites. Calculations by Doyen[6] are also consistent with an atop bond for PF_3 on Ni(111) and calculations by Itoh and Ertl[7] are consistent with a donor–acceptor bond for PF_3 on Ni(111). Calculations by Bagus et al. for PF_3 on Cu_5 clusters also support donor–acceptor bonding. They also note that the π-acceptor capabilities for PF_3 are less than those for CO.[8]

In this work, the chemisorption of PF_3 on Ni(111) is investigated by using the electron stimulated desorption ion angular distribution (ESDIAD) technique, temperature programmed desorption (TPD), Auger electron spectroscopy (AES), and low energy electron diffraction (LEED). ESDIAD has been shown to be extremely useful for determining the orientation of molecular bonds in adsorbed species,[9-11] and the other well-known surface sensitive techniques provide additional valuable information.

One of the motivations for this study was to compare the surface chemistry of PF_3 to that of NH_3 on Ni surfaces. Previous studies of NH_3 adsorption on Ni(110) indicate that NH_3 adsorbs on atop sites.[10,12] Also, electron irradiation of adsorbed NH_3 produces the sub-hydride surface species NH_2[13,14] and NH.[14]

2. Experimental Details

The work described here was performed in a ultrahigh vacuum chamber described in detail elsewhere.[13a] The base pressure for these experiments was less than 3×10^{-11} Torr. High purity (99.99+%) PF_3 (obtained from SCM Specialty Chemicals, Inc.) was transferred under vacuum to a stainless steel bulb where it was further purified by 5 freeze–pump–thaw cycles to remove any entrained gases. PF_3 was admitted directly to the crystal face through a calibrated, collimated, effusion source, thermal molecular beam doser.[15] All gas adsorption took place at a crystal temperature of 85 K. The Ni(111) crystal was oriented with an accuracy of 0.3° and was ground and polished to 0.25 μm surface finish with diamond paste.[16] In situ cleaning of the Ni crystal was carried out by Ar^+ sputtering (typical conditions 2 μA, 2 keV, 45 min) and then annealing at 1050 K for 30 min. Auger spectra following cleaning indicate the following upper limits for impurities in the Auger sampling depth: C, 0.5%; O, 0.2%; P, 1.5%; S, 0.1%.

TPD data were acquired with a multiplexed UTI quadrupole mass spectrometer (QMS) that was set to scan two masses so that each mass was sampled twice every second. For studies of electron-impact-stimulated surface processes, uniform electron bombardment of the crystal face was performed by placing the crystal in a position where 55 eV stray electrons emitted from the QMS thermionic emitter, at a distance of a ~3 cm from the crystal, would strike the crystal surface.

(1) Albert, M. R.; Yates, J. T., Jr. *The Surface Scientist's Guide to Organometallic Chemistry*; American Chemical Society: Washington, DC, 1987.
(2) Nixon, J. F. In *Advances in Inorganic Chemistry and Radiochemistry*; eds, Emeleus, H. J., Sharpe, A. G., Ed.; Academic: New York, 1985; Vol. 29, p 62 and references therein.
(3) Blyholder, G.; Sheets, R. *J. Colloid Interface Sci.* **1974**, *46*, 380.
(4) Ertl, G.; Kuppers, J.; Nitschke, F.; Weiss, M. *Chem. Phys. Lett.* **1977**, *52*, 309.
(5) Nitschke, F.; Ertl, G.; Kuppers, J. *J. Chem. Phys.* **1981**, *74*, 5911.
(6) Doyen, G. *Surf. Sci.* **1982**, *122*, 505.
(7) Itoh, H.; Ertl, G. *Z. Naturforsch.* **1982**, *37*, 346.
(8) Bagus, P. S.; Hermann, K.; Bauschlicher, C. W., Jr. *Ber. Bunsen-Ges. Phys. Chem.* **1984**, *88*, 302.
(9) Madey, T. E.; Netzer, F. P.; Houston, J. E.; Hanson, D. M.; Stockbauer, R. *Desorption Induced by Electronic Transitions, DIET I*; Tolk, N. H., Traum, M. M., Madey, T. E., Tully, J. C., Eds.; Springer Series in Chemical Physics, Vol. 24; Springer-Verlag: Heidelberg, 1983; p 120. Madey, T. E. *Inelastic Ion-Surface Collisions*; Heiland, W., Taglauer, E., Eds.; Springer-Verlag: Heidelberg, 1981; p 80. Madey, T. E. *J. Vac. Sci. Technol.* **1986**, *A4*, 257.
(10) Yates, J. T.; Klauber, C.; Alvey, M. D.; Metiu, H.; Lee, J.; Martin, R. M.; Arias, J.; Hanrahan, C. *Desorption Induced by Electronic Transitions: DIET II*; Brenig, W., Menzel, D., Eds.; Springer-Verlag: Heidelberg, 1985; p 123.
(11) Riedl, W.; Menzel, D. *Desorption Induced by Electronic Transitions: DIET II*; Brenig, W., Menzel, D., Eds.; Springer-Verlag Heidelberg, 1985; p 136.
(12) Klauber, C.; Alvey, M. D.; Yates, J. T., Jr. *Chem. Phys. Lett.* **1984**, *106*, 477.
(13) (a) Klauber, C.; Alvey, M. D.; Yates, J. T., Jr. *Surf. Sci.* **1985**, *154*, 134. (b) Alvey, M. D.; Klauber, C.; Yates, J. T., Jr. *J. Vac. Sci. Technol.* **1985**, *A3*, 1631.
(14) Bassignana, I. C.; Wagemann, K.; Kuppers, J.; Ertl, G. *Surf. Sci.* **1986**, *175*, 22.
(15) Bozack, M. J.; Muehlhoff, L.; Russell, J. N., Jr.; Choyke, W. J.; Yates, J. T., Jr. *J. Vac. Sci. Technol.* **1987**, *A5*, 1.
(16) Alvey, M. D.; Lanzillotto, A.-M.; Yates, J. T., Jr. *Surf. Sci.* **1986**, *177*, 278.

0002-7863/88/1510-1782$01.50/0 © 1988 American Chemical Society

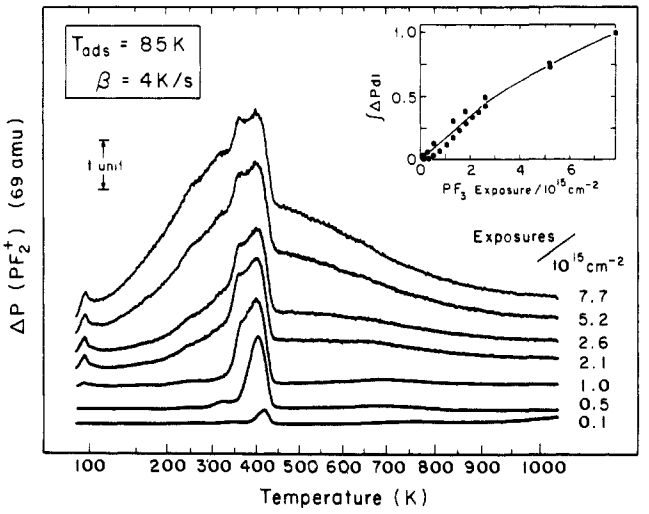

Figure 1. Thermal desorption of PF_3 from Ni(111).

The digital ESDIAD apparatus used here has been described previously.[17] All ESDIAD patterns have had the soft X-ray background removed[17] and have been smoothed with a 49 point two-dimensional, least-squares, quadratic smoothing routine.[16,17] All of the ion patterns were compressed with the application of a 100 V bias between the crystal and the ESDIAD apparatus. The electron energy used for ESDIAD measurements was 300 eV. Because of the sensitivity of adsorbed PF_3 to electron beam damage, ESDIAD measurements were made at very low total electron fluences ($<1 \times 10^{11}$ e^-/cm^{-2}). The apparatus was also used for LEED measurements.[17]

The ESDIAD phenomena reported in this paper are characteristic of the Ni(111) surface and are observed at positions covering 75% of the crystal in its central region.

3. Results

3.1. Temperature Programmed Desorption of PF_3 from Ni(111). Figure 1 shows the TPD traces for various initial exposures of PF_3 on Ni(111). The PF_2^+ ion is displayed because it is the most abundant ion in the cracking pattern of PF_3; however, PF_3^+ was also monitored and showed identical behavior to PF_2^+. F_2 and P_4 were not observed to desorb from the crystal. As seen in Figure 1, after an exposure of 0.5×10^{15} PF_3 cm^{-2}, the single desorption feature at 405 K broadened to lower temperatures and a broad high temperature feature was also observed. As shown in the inset to Figure 1, the coverage of PF_3 did not saturate for the exposures investigated. Using the first-order kinetic analysis by Chan et al.[18] and the full-width at half-maximum of the single low-exposure (0.1×10^{15} cm^{-2}) PF_3 desorption feature yields $E_d = 25.9 \pm 1.7$ kcal mol^{-1}; $\nu_1 = 10^{13\pm1}$ s^{-1} for first-order desorption.

Figure 2 shows the results of a combined AES and TPD study of the desorption of PF_3 from Ni(111). The top panel shows the fraction of PF_3 that remains to desorb based on the total PF_3 that does desorb, versus the crystal temperature for an initial exposure of 5.2×10^{15} PF_3 cm^{-2}. Data for the top panel were obtained by vertically slicing the appropriate TPD curve at the desired temperature, T, and integrating the remaining part of the desorption trace at temperatures greater than T. The bottom panel of Figure 2 was obtained by adsorbing 5.2×10^{15} PF_3 cm^{-2} and then systematically heating the crystal to desorb PF_3. AES data (derivative mode) were then taken by moving the crystal to a new position for each point. The phosphorus 120-eV peak-to-peak intensity was normalized to the nickel 848-eV peak-to-peak intensity. Figure 2 clearly shows that phosphorus remains on the crystal to a high temperature, indicating that about 16% of the adsorbed PF_3 decomposes thermally upon temperature programming. It should be noted that some decomposition of PF_3 occurred in the electron beam during the measurement, so the 16% decomposition is an upper limit for the amount of thermal decomposition for PF_3 adsorbed on Ni(111).

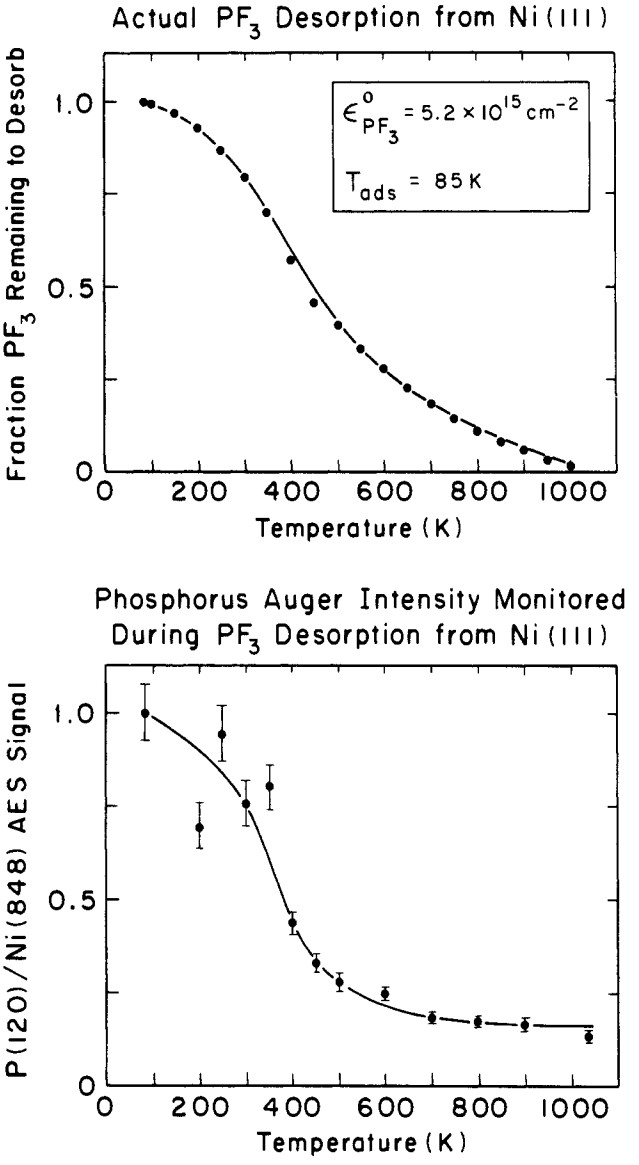

Figure 2. Comparison of the amount of PF_3 leaving the crystal by thermal desorption to the phosphorus remaining on the surface.

3.2. ESDIAD Measurement for PF_3 on Ni(111). Figure 3 shows the F^+ ESDIAD patterns for PF_3 on Ni(111). The left side (a–c) of the figure shows the thermal behavior of the ESDIAD patterns for an exposure of 0.5×10^{15} PF_3 cm^{-2}. In Figure 3a, six F^+ peaks can be seen. By increasing the crystal temperature from 85 K (Figure 3a) to 275 K (Figure 3b), much of the intensity in the peaks is lost (the fine structure is an artifact of the detection system) and an almost uniform F^+ ring ESDIAD pattern is observed. Figure 3c shows that this is a reversible effect. This thermally reversible process has been studied in detail in a previous paper,[19] where Alvey et al. have modeled PF_3 as a two-dimensional, surface rotor and have estimated a barrier to rotation of 80 ± 20 cm^{-1} for isolated PF_3 molecules on Ni(111).[19]

In the right half of Figure 3 (d–f) are the F^+ ESDIAD patterns for an exposure of 2.6×10^{15} PF_3 cm^{-2}. In contrast to the low exposure case (Figure 3a), the six F^+ peaks in Figure 3d are more clearly resolved. Also, the pattern obtained at a substrate temperature of 275 K does not tend toward azimuthal randomness, but a slight broadening of the six F^+ beams is observed. This slight broadening of the ion beams in Figure 3e is also reversible, as seen in Figure 3f. At the higher PF_3 exposure in Figure 3d–f, the PF_3 molecules do not rotate (the hindering potential for rotation in-

(17) Dresser, M. J.; Alvey, M. D.; Yates, J. T., Jr. *Surf. Sci.* **1986**, *169*, *91*; *J. Vac. Sci. Technol.* **1986**, *A4*, 1446.
(18) Chan, C.-M.; Aris, R.; Weinberg, W. H. *Appl. Surf. Sci.* **1978**, *1*, 360.
(19) Alvey, M. D.; Yates, J. T., Jr.; Uram, K. J. *J. Chem. Phys.* **1988**, *87*, 7221.

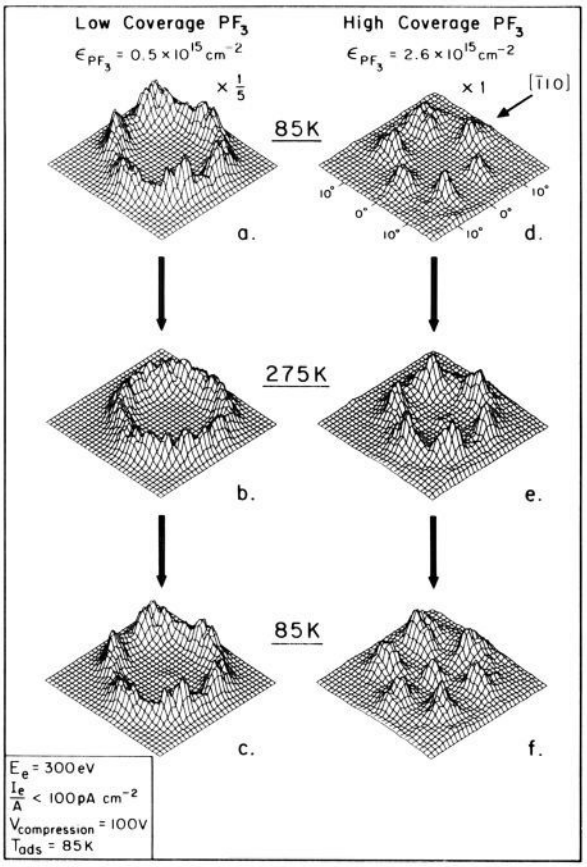

Figure 3. Temperature and coverage dependence of F^+ ESDIAD patterns observed for PF_3 on Ni(111). Estimated PF_3 coverages: low coverage = 0.04 PF_3/Ni(111), high coverage = 0.25 PF_3/Ni(111).

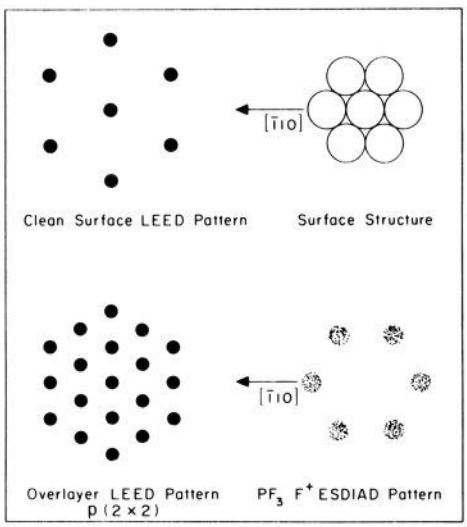

Figure 4. Summary of LEED results and definition of surface directions.

creases) because of intermolecular interactions.[19]

In Figure 3, parts c and f, a central F^+ peak is noticeable. This is due to a very slight amount of electron beam induced fragmentation of PF_3 species to PF species and will be discussed later.

3.3. LEED Studies of PF_3 on Ni(111). Figure 4 summarizes the LEED results obtained for PF_3 on Ni(111). The only LEED pattern observed for this system, other than the clean surface p(1×1), was the PF_3 overlayer p(2×2) pattern. This pattern has also been observed by Nitschke et al.[5] The (2×2) pattern was produced by exposing the crystal to 2.6×10^{15} PF_3 cm^{-2} and then briefly flashing the crystal to 275 K. The (2×2) pattern is consistent with a surface coverage of 0.25 PF_3/Ni. With this as a

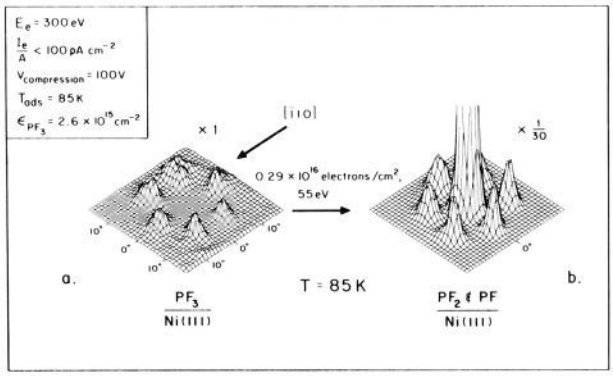

Figure 5. Electron bombardment induced conversion of PF_3 to PF_2 and PF species.

reference point, PF_3 coverages can be estimated from the PF_3 exposures.

Figure 4 also depicts the orientation of the observed F^+ ESDIAD pattern relative to the Ni(111) substrate as determined from the LEED and ESDIAD data.

3.4. Electron Beam Effects of PF_3 on Ni(111). Extensive changes in the F^+ ESDIAD patterns for PF_3 on Ni(111) after electron bombardment have been observed in this study. Electron beam damage for the same system was noted in the LEED study by Nitschke et al.[5]

Figure 5 shows the remarkable change that occurs in the F^+ ESDIAD pattern for PF_3 after exposure to 55 eV electrons. In Figure 5a, the p(2×2) PF_3 overlayer was prepared as indicated in Section 3.3. The adsorbed layer was then uniformly bombarded over the entire crystal face with 0.29×10^{16} electrons cm^{-2}. As shown in Figure 5b, several changes occurred in the F^+ ESDIAD pattern. First, the ion signal increased dramatically, and new features were observed. Most noticeable is the large central beam. In Figure 5b this is plotted off scale so that the less intense features may be seen. The maximum ion count in the central beam of Figure 5b is 500 times greater than the maximum ion count in the 6 F^+ beams in Figure 5a.

The second important change in Figure 5b is the orientation of the six perimeter F^+ beams. When carefully comparing Figure 5b to Figure 5a, it can be seen that the perimeter F^+ beams in Figure 5b are rotated 30° with respect to the F^+ beams in Figure 5a. The maximum F^+ intensity in the perimeter beams in Figure 5b is 60 times greater than the maximum intensity in Figure 5a. If electron bombardment continues past what is shown in Figure 5b, the perimeter beams and the central beam sequentially go through a maximum in F^+ desorption and then decrease.

The electron damage of PF_3 on Ni(111) was further characterized by TPD measurements as shown in Figure 6. For each of the traces in Figure 6 (b–e) a fresh PF_3 layer was adsorbed and them bombarded with 55 eV electrons over the entire surface. Two effects of electron bombardment can be observed in the TPD traces. First, relative to the undamaged PF_3 (Figure 6a), the prominent desorption feature broadens and decreases in intensity. Second, pronounced higher temperature PF_3 desorption features appear.

By using a first-order rate law[20] for the electron impact induced loss of PF_3 in the low-temperature desorption features (below 525 K), a cross section for the loss of these types of PF_3 species can be measured. This measurement is shown in the inset to Figure 6. The total cross section, Q_T, is $\sim 4 \times 10^{-17}$ cm^2 for 55 eV electrons incident on PF_3 adsorbed on Ni(111).

Figure 7 presents the ESDIAD data for PF_3 after electron bombardment of a PF_3 overlayer and subsequent thermal treatment. Figure 7a shows the ESDIAD pattern of a PF_3 layer bombarded at 85 K. This is the same ESDIAD pattern as in Figure 5b. After the crystal is heated to 275 K and then cooled to 85 K, the F^+ ESDIAD pattern in Figure 7b is observed. This

(20) Redhead, P. A. *Can. J. Phys.* **1964**, *42*, 886.

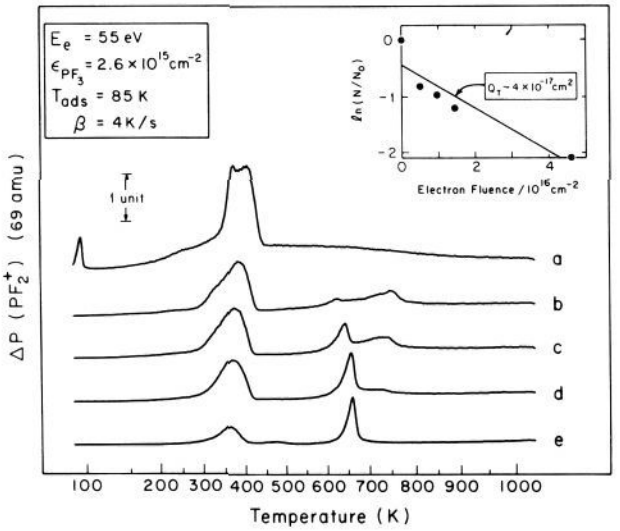

Figure 6. TPD observation of the effect of electron bombardment (55 eV) of PF_3 on Ni(111). The electron fluences, in units of 10^{16} cm^{-2}, are (a) 0.00, (b) 0.50, (c) 0.96, (d) 1.45, (e) 4.62.

pattern appears to be a superposition of two ESDIAD patterns similar to the patterns in Figure 5. Further heating of the crystal to 525 K produces the ESDIAD result shown in Figure 7c. Here only a very small amount of F^+ desorption is observed. It should be noted that after the electron bombardment and heating to 525 K in Figure 7c, only the material that desorbs as PF_3 in the high-temperature TPD features (above 525 K) of Figure 6b is present on the surface.

Observations of the P-Auger line shape were made during desorption from the crystal. No observable changes in line shape were seen. However, the P(120) Auger line overlapped the Ni-(102) Auger line, as well as a Ni diffraction feature, making the measurement difficult. Due to the very large ESD cross section, the F-Auger line was impossible to study in this work; this is a common problem with F-containing adsorbates.

4. Discussion

The combined results of ESDIAD, TPD, AES, and LEED measurements provide models for the chemisorption, orientation, and electron damage products of PF_3 on Ni(111).

4.1. Chemisorption of PF_3. The results of this paper indicate that at temperatures below the desorption temperature (~400 K), PF_3 does not thermally decompose on Ni(111). The ESDIAD patterns observed at 85 K for overlayers that were heated between 85 and 359 K are identical. Nitschke et al.[5] also conclude that PF_3 does not thermally decompose below 400 K.

At higher temperatures, some thermal decomposition of PF_3 does occur. The AES data in Figure 2 show that surface phosphorus remains to high tempertures after PF_3 desorption.

4.2. Orientation of Adsorbed PF_3. From the ESDIAD measurements of the P–F bond direction, combined with the LEED measurements, the adsorption site for PF_3 on Ni(111) can be determined. Figure 3a shows that at a coverage of 0.04 PF_3/Ni and at a coverage of 0.25 PF_3/Ni (Figure 3d) the predominant orientation of P–F bonds is the same. The differences between parts a–c and d–f of Figure 3 are due to the fact that at the low coverage, isolated PF_3 molecules undergo hindered rotation, while at higher coverages, rotation is not possible due to intermolecular interactions.[19]

Figure 4 shows the orientation of the F^+ ESDIAD beams relative to the Ni substrate determined from LEED and ESDIAD measurements. In determining an adsorption site that is consistent with the known bonding of PF_3 (see Introduction) and the experimental data from this study, only one type of site is allowed. The calculations by Doyen,[6] the analogy to PF_3 bonding in transition-metal compounds,[2] and the ESDIAD data all favor an atop chemisorption site. By placing the PF_3 molecule on an atop Ni site, the ESDIAD results indicate that the P–F bonds are

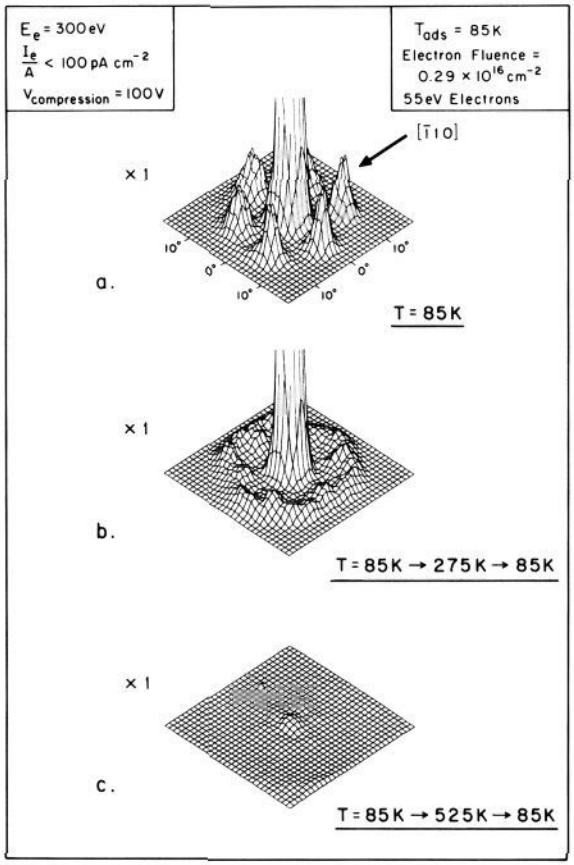

Figure 7. ESDIAD observation of thermal effects in electron bombarded PF_3 on Ni(111).

directed over neighboring Ni atoms. Placing the azimuthally oriented PF_3 molecule elsewhere on the surface directs P–F bonds along directions that are unsymmetrical with respect to the site. Figure 8 shows that there are two atop azimuthal orientations that direct P–F bonds over neighboring Ni atoms. Thus, the observed F^+ ESDIAD pattrn for PF_3 is a superposition of both of these orientations. From the p(2×2) LEED patterns seen in this study, and by Nitschke et al.,[5] the packing of the PF_3 overlayer shown in Figure 8 has also been determined.

4.3. Electron Damage of PF_3 on Ni(111). Figures 5–7 show the effect of electron damage of PF_3 on the observed ESDIAD patterns and the TPD data. A striking change in the ESDIAD pattern is observed when PF_3 is irradiated by electrons as in Figure 5. The production of a central F^+ beam and the 30° rotation of the perimeter F^+ beams can be understood as being due to the electron induced formation of PF_x species ($x < 3$). This production of PF_x species is a direct analogy to the electron induced production of NH_x species from NH_3 on Ni(110).[13,14]

First, consider the six perimeter F^+ ion beams. These are probably due to F^+ emission from PF_2 species on the surface. PF_2 is known to be a twofold bridging ligand in inorganic chemistry.[2] Placing PF_2 in the three types of bridging sites on the Ni(111) surface, as shown in Figure 8, will give an ESDIAD pattern for the six perimeter F^+ beams that is consistent in azimuthal orientation with the data observed in Figure 5b (or Figure 7a).

The next feature in Figure 5b (or Figure 7a) to be addressed is the intense central F^+ beam. The species responsible for this beam must be bound with a chemical bond oriented normal to the surface. A PF species with the F atom directed normal to the surface meets this description; however, adsorbed fluorine might also produce a normal F^+ beam. The data presented in Figures 5, 6, and 7 suggest that the central feature in Figure 5b (or Figure 7a) is probably F^+ emission from PF species. Total decomposition of the PF_3 layer by electron bombardment gives no F^+ ESDIAD patterns, even though P(ads) and F(ads) are still on the surface. The TPD traces in Figure 6 show that after

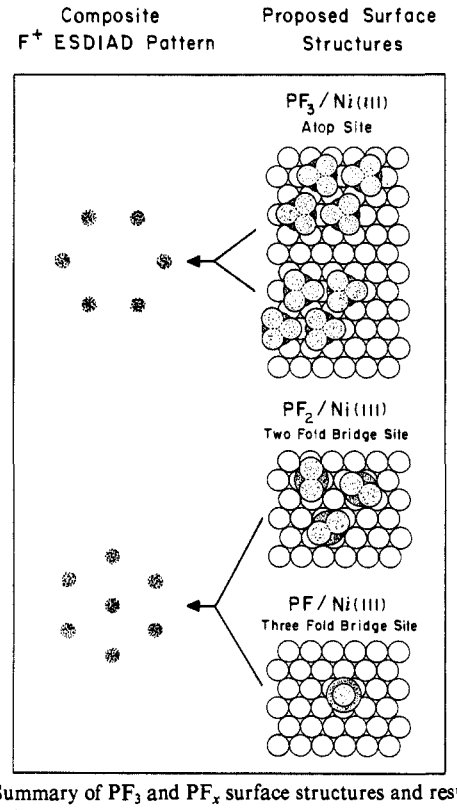

Figure 8. Summary of PF_3 and PF_x surface structures and resultant F^+ ESDIAD patterns.

electron bombardment to produce essentially total PF_3 decomposition, PF_3 desorbs from the surface above 525 K, indicating that PF_3 fragments such as P and F are still on the surface and able to recombine to produce PF_3 at temperatures above 525 K. Hence, on this basis it is most likely that the central F^+ beam in Figure 5b (or Figure 7a) is due to adsorbed PF. This argument is of course open to criticism and can eventually be substantiated by various surface spectroscopies; however, from the data obtained in this work it is a reasonable assignment. The authors have postulated that the PF species will bond in a threefold coordinated site, directing the P–F bond normal to the surface.

Now that an assignment of all the F^+ beams to PF_3(ads), PF_2(ads), and PF(ads) has been made, it can be seen that Figure 5b (or Figure 7a) is a composite of F^+ beams from PF_2 and PF species produced by the electron bombardment of PF_3 on Ni(111). This is depicted in Figure 8.

4.4. Cross Section for F^+ Production from PF_x Species. Another issue to be addressed is the increase in F^+ emission for the PF_2 and PF species relative to the F^+ emission from PF_3. One explanation is that the trajectories for F^+ ions from PF_2 and PF are along angles further from the surface than F^+ trajectories from PF_3. Ion trajectories far from the surface are less affected by Hagstrum neutralization (exponential decrease in rate of neutralization with increasing distance from surface) than trajectories close to the surface.[21] Using bond data for the model compound $Ni(PF_3)_4$[22] for PF_3, and assuming that similar bond geometry is appropriate for PF_3 chemisorbed on the Ni(111) surface, indicates that the polar angle for the P–F bond is 61° from the surface normal. The authors are not aware of similar data for the PF_2 species; however, it is reasonable to assume that the bond angle lies near a pure tetrahedral bond arrangement, yielding a polar angle of 55°. PF is proposed to bond with the PF bond direction normal to the surface, as based on the observed ESDIAD patterns. From the geometries and the effect of neutralization of ion trajectories close to the surface, it would be expected that the F^+ ion pattern from PF would be most intense, followed by PF_2, and then PF_3. Qualitatively, these geometric effects (influencing neutralization of F^+ ions) could explain the relative F^+ yields. Of course, other factors affecting the excitation and de-excitation pathways for the different species could also be involved in causing the observed difference in ion yields.

5. Summary

In this work, PF_3 is observed to adsorb molecularly at 85 K on Ni atop sites in the Ni(111) surface. The PF_3 is azimuthally oriented so that individual P–F bonds are directed over neighboring Ni atoms. Since there are two such orientations on the Ni(111) crystal plane, the observed ESDIAD patterns contain six F^+ beams in a hexagonal pattern. In the low coverage limit, PF_3 exhibits an activation energy of desorption of 25.9 ± 1.7 kcal mol^{-1}.

PF_3(ads) may be converted to PF_2(ads) and PF(ads) by means of electron bombardment. PF_2 adsorbs on twofold Ni bridging sites, yielding six unique P–F bond directions. The hexagonal, six beam F^+ ESDIAD pattern observed for PF_2 is rotated 30° from the hexagonal, six beam F^+ ESDIAD pattern observed for PF_3. PF is postulated to bind in a threefold Ni bridging site, yielding a normal P–F bond orientation.

The apparent F^+ ionic cross section for PF_x species increases in the order $Q^+_{PF_3} < Q^+_{PF_2} < Q^+_{PF}$. This may be accounted for, in part, by the decreasing polar angle from the surface normal of the P–F bond in this series.

On the basis of this work for PF_3/Ni(111) and the work on NH_3/Ni(110),[13,14] it appears that electron bombardment may be used to produce surface species such as PF_2, PF, NH_2, and NH from their precursor molecules. New surface species produced in this manner may be useful in studying surface reactions and chemically modified surfaces.

Acknowledgment. We gratefully acknowledge support of this work by a grant from the Air Force Office of Scientific Research under contract No. 86-0107. We would also like to thank Dr. I. D. Brown for investigating crystal structures containing PF_2.

Registry No. PF_3, 7783-55-3; PF_2, 20762-58-7; PF, 16027-92-2; Ni, 7440-02-0.

(21) Madey, T. E.; Yates, J. T., Jr. *J. Vac. Sci. Technol.* **1971**, *8*, 525.
(22) Almenningen, A.; Anderson, B.; Astrup, E. E. *Acta Chem. Scand.* **1970**, *24*, 1579.